Journal of Electronic Materials, Vol. 23, No. 8, 1994

Solid State Intermetallic Compound Growth Between Copper and High Temperature, Tin-Rich Solders—Part II: Modeling

K.L. ERICKSON, P.L. HOPKINS, and P.T VIANCO

Engineering Sciences Center & Center for Solder Science and Technology, Sandia National Laboratories, Albuquerque, NM 87185

The solder/base metal interfacial chemistry characterizing solder joints impacts the manufacturability and reliability of electronic components. A model was developed to predict the long-term diffusion-controlled growth of interfacial intermetallic compound layers using short-term experimental data. The model included terms for both constant and variable diffusion coefficients. Application of the model was demonstrated using parameter values for 100Sn/Cu system and comparing calculated layer thicknesses with the experimentally observed values. The early time data for the 100Sn/Cu system that were used to predict growth at longer times were characterized using a variable diffusion coefficient that was an empirical function of layer thickness.

Key words: Interfacial diffusion, intermetallic growth, solder

INTRODUCTION

The growth of intermetallic layers occurs by displacement of the interfaces between layers that results from diffusion and interfacial reaction of the constituents of the layers. Analytical solutions to the diffusion and interface displacement equations are available for analyzing simple systems in which:

- diffusion of the constituents can be represented by Fick's law with constant diffusion coefficient;
- interfacial reactions are sufficiently fast so that local chemical equilibrium essentially exists at both sides of each interface, and constituent concentrations at both sides can be considered constant, although generally they are not equal;
- all layers grow simultaneously and have negligible initial thicknesses;
- constituent diffusion and interface displacement are not hindered by finite material boundaries; and
- diffusion and layer growth can be considered one-dimensional.

The objective of the modeling and corresponding code development work was to provide numerical tools necessary for analysis of more complex systems and for predicting intermetallic growth during service in which:

- diffusion of constituents occurs by multiple mechanisms having variable diffusion coefficients;
- interfacial chemical reactions are slow enough to be rate-limiting;
- all layers do not grow simultaneously, due to different nucleation rates, and initial film thicknesses are not negligible;
- constituent diffusion and interface displacement are hindered by finite material boundaries;
- the temperature and, therefore, the diffusion coefficients vary substantially during layer growth; and
- constituent diffusion and layer growth occur in more than one dimension.

(Received March 1, 1994; Revised March 14, 1994)

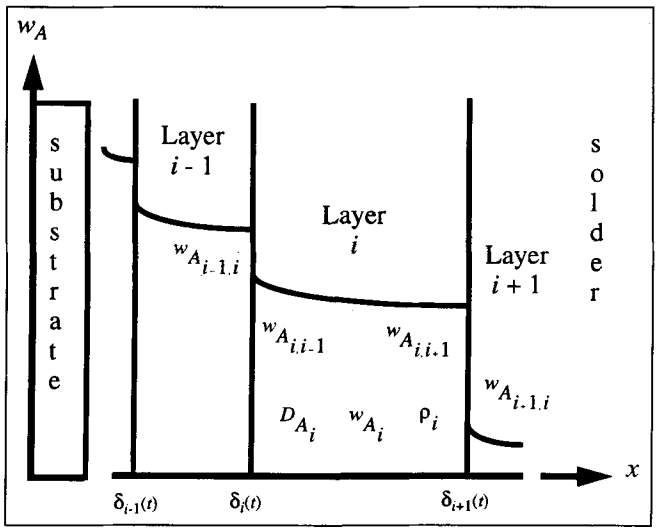

Fig. 1. Schematic diagram of intermetallic layer growth between substrate and solder.

A summary of the modeling and corresponding code development work is given below. The equations governing the basic phenomena controlling intermetallic growth are described first. Analytical and numerical solution of the equations is then discussed, and the use of the numerical model is illustrated by application to experimental data for the 100Sn/Cu system. This work primarily addresses the long-term growth of intermetallic layers that were previously formed by short-term contact between a metal substrate and molten solder and subsequent rapid solidification of the solder.

MODEL

This work is based on a one-dimensional, multilayer system involving a binary set of interacting constituents, such as Cu and Sn, and in each layer, the diffusion of either constituent can be rate-controlling. The model consists of a basic set of material balance equations for each layer and displacement equations for the interfaces on each side of the layer. The material balance equations describe bulk diffusion of the rate-controlling constituent in each layer. In addition to bulk diffusion, the material balance equations can accommodate terms for additional diffusion mechanisms, such as grain boundary diffusion, and terms for rate-limiting interfacial reactions. Analogous material balance equations can be included to describe diffusion of trace constituents as appropriate.

A substrate solder system in which n intermetallic layers form and grow between the substrate and bulk solder is shown schematically in Fig. 1. Let the substrate form the left boundary of the system, and solder the right boundary. Let i = 1,2,3,...,n denote the sequence of intermetallic layers growing from left to right. That is, i = 1 denotes the layer adjacent to the right edge of the substrate, and i = n denotes the layer adjacent to the left edge of the solder. Furthermore, let T denote the temperature, t denote time, x denote position with respect to an origin fixed in space, $\delta_i(t)$ the position of the interface between layer i–1 and layer i, and $\Delta_i(t)$ the thickness of layer i

$$\Delta_i(t) = \delta_{i+1}(t) - \delta_i(t) \tag{1}$$

Then, for $\delta_i(t) < x < \delta_{i+1}(t)$, the material balance for the rate-controlling constituent in each layer is given by

$$\frac{\partial w_{A_i}}{\partial t} = \frac{\partial}{\partial x}\left(D_{A_i} \frac{\partial w_{A_i}}{\partial x} \right) \tag{2}$$

where w_{A_i} denotes the mass fraction of the rate-controlling constituent in layer i, and D_{A_i} denotes the constituent's diffusion coefficient, which can be a function of x, t, w_{A_i}, T, and $\Delta_i(t)$, and can be specified accordingly. In general, the temperature T can be a function of x and t, which also can be specified.

When constituent diffusion and interface displacement are not hindered by finite material boundaries, and the rate R_i of interfacial chemical reaction is sufficiently fast, local chemical equilibrium exists at the interface, and the concentrations of the diffusing constituents in layer i are essentially constant at $\delta_i(t)$. Therefore, at $\delta_i(t)$, the boundary condition for Eq. (2) is

$$\left(w_{A_i}\right)_{\delta_i^r} = w_{A_{i,i-1}} = \text{constant} \tag{3}$$

and if local equilibrium exists at $\delta_{i+1}(t)$, the boundary condition is

$$\left(w_{A_i}\right)_{\delta_{i+1}^l} = w_{A_{i,i+1}} = \text{constant} \tag{4}$$

where $w_{A_{i,i-1}} \neq w_{A_{i,i+1}}$, and superscripts l and r denote values at the left and right sides of the interface, respectively. The initial condition for Eq. (2) is

$$w_{A_i}(x,0) = f_i(x) \tag{5}$$

where $f_i(x)$ is known or assumed.

When the rate R_i of interfacial reaction is slow enough to preclude local equilibrium at the interface, the constant concentration boundary conditions given by Eqs. (3) and (4) must be replaced by flux-type boundary conditions given by

$$-\rho D_{A_i}\left(\frac{\partial w_{A_i}}{\partial x}\right)_{\delta_i^r} = R_i^r \tag{6}$$

$$-\rho_i D_{A_i}\left(\frac{\partial w_{A_i}}{\partial x}\right)_{\delta_{i+1}^l} = R_i^l \tag{7}$$

Furthermore, when constituent diffusion encounters a finite material boundary, the boundary condition for Eq. (2) becomes the zero flux condition at that boundary.

The displacement of each interface is given by

$$\left[\rho_{i-1}\left(w_{A_{i-1}}\right)_{\delta_i^l} - \rho_i\left(w_{A_i}\right)_{\delta_i^r}\right]\frac{d\delta_i}{dt} = -\rho_{i-1} D_{A_{i-1}}\left(\frac{\partial w_{A_{i-1}}}{\partial x}\right)_{\delta_i^l} + \rho_i D_{A_i}\left(\frac{\partial w_{A_i}}{\partial x}\right)_{\delta_i^r} \tag{8}$$

where ρ_i denotes the mass density of layer i. The

initial condition for Eq. (10) is

$$\delta_i(t = 0) = \delta_i^0 = \text{a constant} \quad (9)$$

If D_{A_i} and ρ_i have constant values in each layer, if the boundary conditions given by Eqs. (3) and (4) apply, and if δ_i^0 in Eq. (9) is essentially zero, then Eqs. (2) and (8) can be solved analytically for each layer, as discussed by Jost.[1] In each layer, w_{A_i} is given by

$$w_{A_i} = \left(w_{A_i}\right)_{\delta_i^f} - H_i\left[\frac{\text{erf}(\gamma_i) - \text{erf}(\eta_i)}{\text{erf}(\gamma_i) - \text{erf}\left(\gamma_{i+1}\sqrt{\phi_{i+1}}\right)}\right] \quad (10)$$

where

$$\eta_i = \frac{x}{2\sqrt{D_{A_i} t}} \quad (11)$$

$$\phi_i = \left(\frac{\rho_i}{\rho_{i-1}}\right)\frac{D_{A_i}}{D_{A_{i-1}}} \quad (12)$$

and

$$H_i = \rho_i\left[\left(w_{A_i}\right)_{\delta_i^f} - \left(w_{A_i}\right)_{\delta_{i+1}^f}\right] \quad (13)$$

The displacement of each interface is given by

$$\delta_i(t) = 2\gamma\sqrt{D_{A_i} t} \quad (14)$$

where

$$\gamma_i = \quad (15)$$

$$\frac{1}{\sqrt{\pi\phi_i}}\frac{1}{h_i}\left[\frac{\sqrt{\phi_i}H_i\exp(-\gamma_i^2)}{\text{erf}(\gamma_i) - \text{erf}\left(\gamma_{i+1}\sqrt{\phi_{1+1}}\right)} - \frac{H_{i-1}\exp(-\phi_i\gamma_i^2)}{\text{erf}(\gamma_{i-1}) - \text{erf}\left(\gamma_i\sqrt{\phi_i}\right)}\right]$$

and

$$h_i = \rho_{i-1}\left(w_{A_{i-1}}\right)_{\delta_i^f} - \rho_i\left(w_{A_i}\right)_{\delta_i^f} \quad (16)$$

Equations (10)–(16) are useful for some data analysis and for verifying numerical techniques. It should be noted that in Eq. (17) for γ_i, terms involving γ_{i-1} and γ_{i+1} also appear. Therefore, the equations for γ_i must be solved simultaneously, and since the equations are very nonlinear, numerical solution is necessary.

In this work, the numerical approach adopted to solve the system of coupled diffusion and interface displacement equations given by Eqs. (2) and (8) for each layer was the method of lines,[2] which uncouples the spatial and temporal discretization of the partial differential equations. In this application, the spatial discretization is represented by finite differences, which results in a set of coupled, first-order, ordinary differential equations in time. These are solved in turn by an efficient library ordinary differential equation (ODE) solver that determines the time stepping internally to maintain stability.

The implicit solution procedure of the ordinary differential equation solver uses a variable order (one through five) backward difference formulation.[3,4] Baer's[5] implementation of the method of lines for solving reactive diffusion equations was adopted in this work. This implementation includes an adaptive meshing scheme[6] that automatically resolves steep mass fraction gradients and will return to a coarser grid as the gradient relaxes. A transformation of the spatial coordinate x given by

$$\bar{x}_i = \frac{x - \delta_i(t)}{\Delta_i(t)} \quad (17)$$

was used to circumvent the need to remesh the growing (or) shrinking layers. The numerical solution of Eqs. (2) and (8) was compared with the analytical solution for systems involving two, three, and five layers. The analytical solution is based on zero initial thickness of the intermetallic layers and local chemical equilibrium between constituents at the interfaces between layers. The numerical solutions for the same conditions were in good agreement with the analytical results, as indicated in Fig. 2, which compares the analytical and numerical results for a five-layer system.

COMPARISON OF MODEL AND EXPERIMENT

The 100Sn/Cu system discussed above was chosen to illustrate some applications of numerical modeling of intermetallic layer growth. It was shown above that in the 100Sn/Cu system, growth of the Cu_3Sn and Cu_6Sn_5 intermetallic layers was approximately proportional to the square root of time, and, therefore, was consistent with bulk diffusion of Cu and Sn controlling growth of the layers. A more detailed analysis using numerical modeling was done to compare the experimental data for intermetallic growth with results calculated assuming growth was controlled by bulk diffusion of Cu or Sn. The analyses were done using a four-layer model that consisted of Cu, Cu_3Sn, Cu_6Sn_5, and Sn layers, denoted by sub -

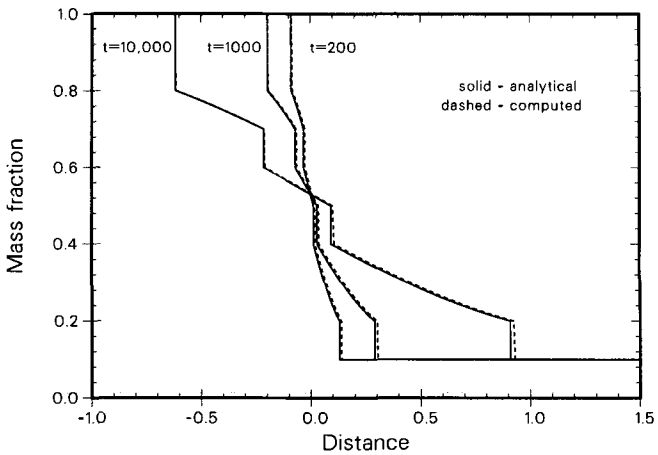

Fig. 2. Comparison of analytical and numerical solutions for a five-zone system.

Table I. Interfacial Concentrations and Mass Densities

Layer	$w_{i,i-1}$	$w_{i,i+1}$	ρ_i (g/cm²)
(1) Cu	1.000	1.000	8.9
(2) Cu_3Sn	0.623	0.605	9.0
(3) Cu_6Sn_5	0.410	0.400	8.4
(4) Sn	0.000	0.000	7.3

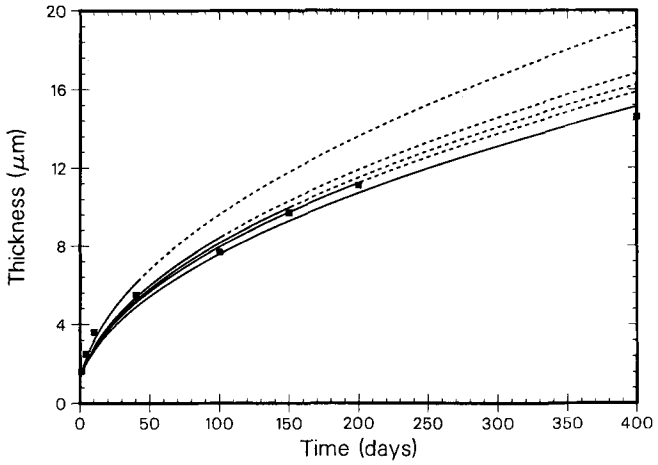

Fig. 3. Cu_3Sn layer thicknesses calculated using a constant diffusion coefficient.

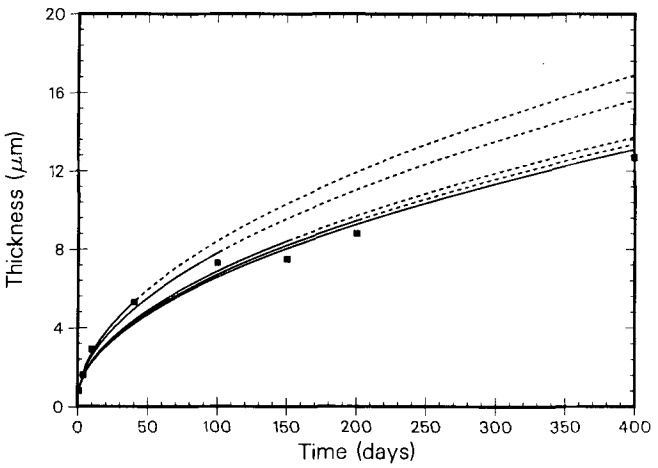

Fig. 4. Cu_6Sn_5 layer thicknesses calculated using a constant diffusion coefficient.

scripts 0,1,2, and 3, respectively. Since the experimental data indicated that diffusion of Sn into the Cu substrate and diffusion of Cu into the bulk Sn were negligible, two diffusion equations [Eq. (2)] were required, one for each of the Cu_3Sn and Cu_6Sn_5 layers, and three interface displacement equations, one each for the interface $\delta_1(t)$ between Cu and Cu_3Sn, $\delta_2(t)$ between Cu_3Sn and Cu_6Sn_5, and $\delta_3(t)$ between Cu_6Sn_5 and Sn. However, the experimental data did not indicate which constituent controlled bulk diffusion in the intermetallic layers.

Since the choice of constituent does not alter the overall effect of bulk diffusion, the analyses were based on Cu being the diffusion controlling constituent. Local equilibrium was assumed at each side of $\delta_1(t)$, $\delta_2(t)$, and $\delta_3(t)$. The constant concentration boundary conditions given by Eqs.(3) and (4) were then evaluated from the Cu-Sn phase diagram and are shown in Table I, which also includes the mass density of each layer. The initial thicknesses of the intermetallic layers were taken from the experimental data for day one (1.6 and 0.9 microns for Cu_3Sn and Cu_5Sn_6, respectively).

The diffusion coefficients in both intermetallic layers were initially assumed constant. The experimental data for layer growth at times from 1 to 40 days were then used to determine values for D_{A_i} that reasonably reproduced the experimental data. Using those values, growth of the Cu_3Sn and Cu_6Sn_5 layers was predicted for times to 400 days and compared with the corresponding experimental data. Analogous calculations were then repeated using the experimental data from 1 to 100, 1 to 150, 1 to 200, and 1 to 400 days to determine the values for D_{A_i}. The results are summarized in Fig. 3 and Fig. 4 for the Cu_3Sn and Cu_6Sn_5 layers, respectively, at 170°C. The solid portion of each curve indicates the time interval in which the experimental data were used to evaluate the diffusion coefficients, and the dashed portion indicates the time interval in which the calculations were continued to longer times. The diffusion coefficients corresponding to each curve for Cu_3Sn and Cu_6Sn_5 are shown in Table II. The results generally indicate that the experimental data are consistent with a bulk diffusion mechanism, but the diffusion coefficient is probably not constant. During early times, diffusion appears to be faster relative to later times. Similar effects have been reported previously. Kofstad[7] used the term "enhanced diffusion" to indicate effects which could be attributed to grain boundary diffusion, residual strain, and poor crystallization during early layer growth.

To empirically account for the effects of enhanced diffusion, an analogous series of calculations was

Table II. Constant Cu Diffusion Coefficients Determined for the Cu_3Sn and Cu_6Sn_5 Layers at 170°C

Time from Day 1 to Day	D_A (Cu_3Sn) $\times 10^8$ (cm^2/day)	D_A(Cu_6Sn_5) $\times 10^7$ (cm^2/day)
40	9.0	1.5
100	7.5	1.2
150	6.8	1.0
200	6.5	1.0
400	6.0	0.9

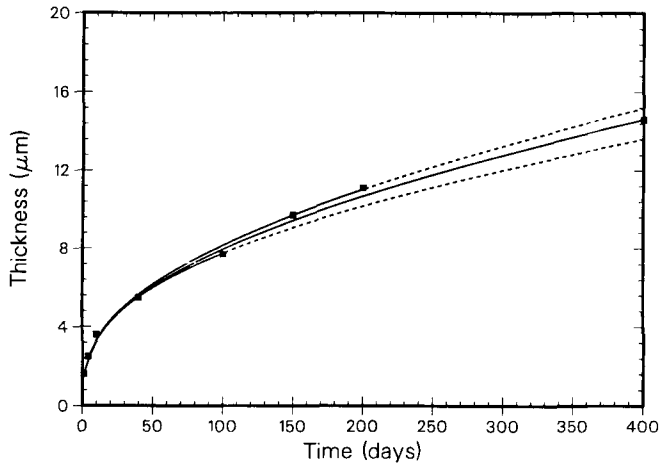

Fig. 5. Cu_3Sn Layer thicknesses calculated using a variable diffusion coefficient (Eq. 18).

done using a variable diffusion coefficient $\overline{D}_{A_i}$ given by

$$\overline{D}_{A_i} = D_{A_i}\left(1+\frac{D'_{A_i}}{D_{A_i}}\exp(-\lambda_i\Delta_i)\right) \quad (18)$$

where D'_{A_i} is an early-time diffusion coefficient that decays with the layer thickness $\Delta_i(t)$, and λ_i is the decay constant. The numerical results are compared with the experimental data in Fig. 5 and Fig. 6. The corresponding values for D_{A_i}, D'_{A_i}, and λ_i are given in Table III. Using Eq. (18), the agreement between experimental and calculated values is considerably improved. This improvement is further illustrated in Fig. 7 and Fig. 8 which compare the numerical results obtained using a constant diffusion coefficient and the variable coefficient given by Eq. (18). The above results indicate that layer growth is consistent with a bulk diffusion mechanism involving a variable diffusion coefficient that probably should reflect some enhanced diffusion during early layer growth. Furthermore, similar analyses with the data from experiments at 135 and 205° C gave analogous results.

CONCLUSIONS

The comparison between modeling and experimental results discussed above for the 100Sn/Cu system demonstrated that numerical modeling can be a valuable tool in the analysis of intermetallic layer growth. In particular, numerical modeling can account for effects that cannot be modeled analytically, such as variable diffusion coefficients, multiple diffusion mechanisms, and rate-limiting interfacial reaction rates. In the 100Sn/Cu system, the comparison between modeling and experimental results showed that intermetallic layer growth is consistent with a bulk diffusion mechanism involving a variable diffusion coefficient that probably should reflect some enhanced diffusion during early layer growth. Furthermore, the enhanced diffusion can be accounted for empirically using a variable diffusion coefficient that is a function of layer thickness. These effects are

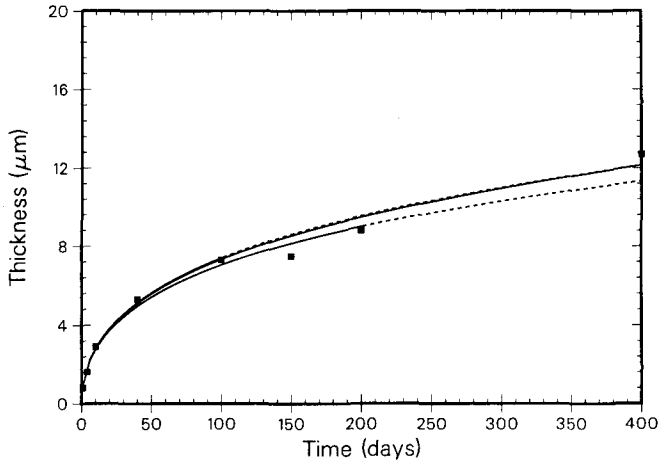

Fig. 6. Cu_6Sn_5 layer thicknesses calculated using a variable diffusion coefficient [Eq. (18)].

Table III. Values for D_A, D'_A, and λ_i (Eq. 18) for the Cu_3Sn and Cu_6Sn_5 Layers at 170°C

Layer	Time Interval from Day 1 to Day	$D_A \times 10^8$ (cm²/day)	$D'_A \times 10^7$ (cm²/day)	$\lambda_1 \times 10^3$ (cm⁻¹)
Cu_3Sn	100	3.5	1.6	3.5
	200	4.5	1.4	3.8
	400	4.3	1.4	3.8
Cu_6Sn_5	100	0.4	1.8	1.9
	200	0.4	1.8	2.1
	400	0.5	1.7	2.1

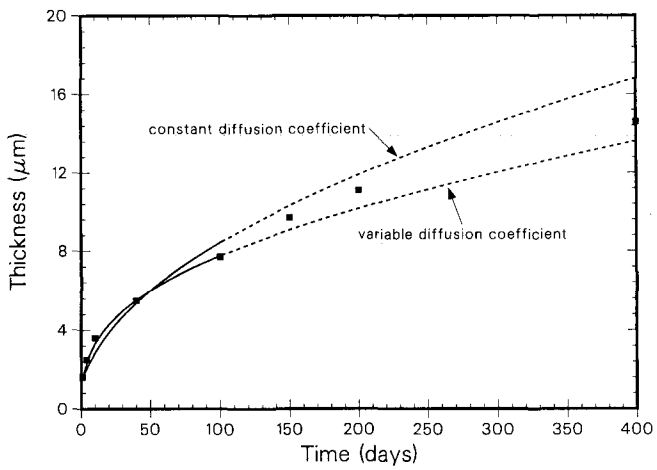

Fig. 7. Comparison of Cu_3Sn layer thicknesses calculated using constant and variable [Eq. (18)] diffusion coefficients.

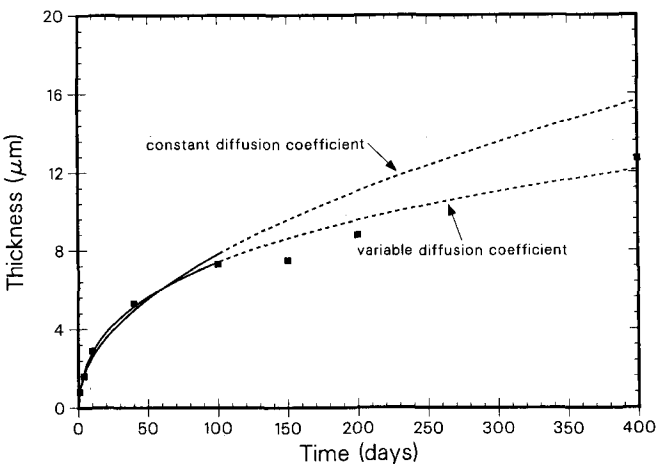

Fig. 8. Comparison of Cu_6Sn_5 layer thicknesses calculated using constant and variable [Eq. (18)] diffusion coefficients.

important when using data from short term isothermal experiments to evaluate diffusion coefficients to be used for predicting long-term layer growth under nonisothermal service conditions. The results are also important when trying to predict the nucleation of additional phases during growth of the original layers.

ACKNOWLEDGMENTS

The authors gratefully acknowledge the technical assistance provided by M.R. Baer and J.R. Torczynski of Sandia National Laboratories. This work performed at Sandia National Laboratories supported by tlhe U. S. Department of Energy under contract number DE-AC04-94-A185000.

REFERENCES

1. W. Jost, *Diffusion in Solids, Liquids, Gases,* (New York: Academic Press, 1960), p. 69.
2. J.M. Hyman, *Method of Lines Approach to the Numerical Solution of Conservation Laws, LA-UR-79-837,* (Los Alamos, NM: Los Alamos Scientific Laboratory, 1979).
3. L.F. Shampine and H.A. Watts, *DEPAC-Design of a User Oriented Package of ODE Solvers, SAND79-2374,* (Albuquerque, NM: Sandia National Laboratories, 1980).
4. A.C. Hindmarsh, *ODE Solvers for Use with the Method-of-Lines, UCRL-85293 (Rev. 1),* (Livermore, CA: Lawrence Livermore National Laboratories, 1981).
5. R.J. Gross, M.R. Baer, and M.L. Hobbs, *XCHEM-1D A Heat Transfer/Chemical Kinetics Computer Program for Multilayered Reactive Materials, SAND93-1603,* (Albuquerque, NM: Sandia National Laboratories, 1993).
6. M.R. Baer, R.E. Benner, R.J. Gross, and J.W. Nunziato, *Lectures in Applied Mechanics,* 24 (1986).
7. P. Kofstad, *High Temperature Oxidation of Metals,* (New York: John Wiley & Sons, Inc., 1966), p. 140.